BREAKDOWN OF LONG-LIVED COLLISION DYNAMICS IN THE REACTIONS OF CHLORINE ATOMS WITH ALKYL IODIDES

S.M.A. HOFFMANN, D.J. SMITH, A. GONZÁLEZ UREÑA [+] and R. GRICE
Chemistry Department, University of Manchester, Manchester M13 9PL, UK

Received 17 January 1984; in final form 15 March 1984

Differential reaction cross sections have been measured as a function of initial translational energy for the I atom abstraction reactions of Cl atoms with CH_3I, C_2H_5I, C_3H_7I molecules. At lower initial translational energy, long-lived collision dynamics are observed which persist at higher initial translational energy for smaller impact parameter collisions but a direct stripping component with a higher product translational energy appears for collisions at the largest impact parameters.

1. Introduction

The breakdown of long-lived collision dynamics with increasing collision energy provides a direct means of studying the extent of energy randomisation in a polyatomic system. The osculating complex model [1] assumes a distribution of collision lifetimes which decays exponentially with time and thus assumes that a statistical description of the collision complex behaviour may be applied when the mean lifetime of the complex becomes comparable to its rotational period. Indeed the osculating complex model has been used to describe the exoergic abstraction of I atoms from CH_3I molecules by F atoms [2] as a function of collision energy. In contrast the endoergic abstraction by Br atoms [3] shows rebound behaviour. The near thermoneutral abstraction of I atoms from alkyl iodide molecules by Cl atoms might therefore be expected. to exhibit transitional behaviour with the extent of energy randomisation being influenced by the number of internal degrees of freedom of the alkyl radical. Here the abstraction of iodine from a homologous series of alkyl iodides by chlorine atoms has been studied as a function of collision energy in order to test this expectation:

$$Cl + RI \rightarrow ICl + R\,, \quad R = CH_3, C_2H_5, C_3H_7\,. \qquad (1)$$

2. Experimental

The apparatus was the same as that employed in a previous study of Cl + I_2 reactive scattering [4] using a supersonic Cl atom beam produced from a high-pressure microwave discharge source [5]. The velocity of the Cl atom beam was varied over the range 1150–1950 m s^{-1} by varying the proportion of Cl_2 diluted in excess He buffer gas and also by using Ne buffer gas. The highest velocity corresponds to ≈5% Cl_2 in in He and the lowest velocity to ≈10% Cl_2 in Ne. The reactively scattered ICl product was measured by a rotatable mass spectrometer detector using cross-correlation time-of-flight analysis [6] to determine the product velocity distribution at each laboratory scattering angle.

3. Results

The laboratory angular distributions of ICl reactive scattering from Cl + CH_3I and C_2H_5I are shown in figs. 1 and 2. In both cases the right-hand-most distri-

---

[+] Permanent address: Departamento Quimica Fisica, Facultad de Ciencias Quimicas, Universidad Complutense, Madrid 3, Spain.

0 009-2614/84/$ 03.00 © Elsevier Science Publishers B.V.
(North-Holland Physics Publishing Division)

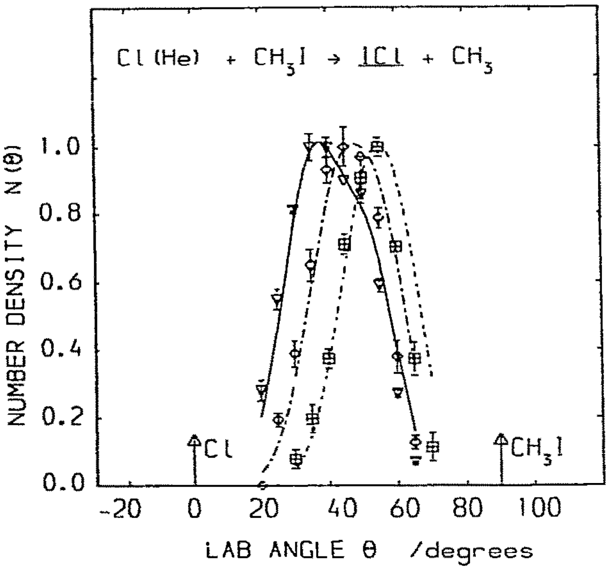

Fig. 1. Laboratory angular distributions (number density) of reactively scattered ICl from Cl + CH_3I as a function of initial translational energy $E = 56$ kJ mol^{-1} (inverted open triangles), $E = 41$ kJ mol^{-1} (open diamonds) and $E = 22$ kJ mol^{-1} (open squares).

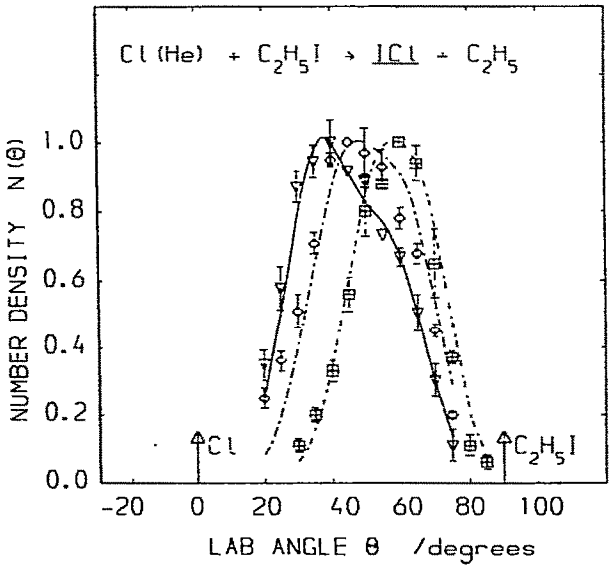

Fig. 2. Laboratory angular distributions (number density) of reactively scattered ICl from Cl + C_2H_5I as a function of initial translational energy.

bution, shown by open squares and a broken line, corresponds to the lowest collision energy $E \approx 22$ kJ mol^{-1}, the left-hand-most distribution, shown by open inverted triangles and a solid line, to the highest collision energy $E \approx 55$ kJ mol^{-1}, and the centre distribution, shown by open diamonds and a broken line, to intermediate collision energy $E \approx 40$ kJ mol^{-1}. Product velocity distributions have also been measured at each laboratory scattering angle for each of these angular distributions. A contour map of the laboratory flux distribution for ICl product from Cl + C_2H_5I at the highest collision energy is shown in fig. 3 together with the nominal Newton diagram. The kinematic analysis of these data has been carried out using the stochastic method of Entemann [7] with a two-component mechanism consisting of a long-lived collision complex with mild forward and backward peaking and a sharply forward peaked stripping component. The centre-of-mass angular distributions $T(\theta)$ and product translational energy distributions $P(E')$ obtained from the analysis of the Cl + C_2H_5I data at the highest collision energy are shown in fig. 4. The product translational energy distribution obtained from the RRKM AM model [8] for the long-lived complex component, shown by a solid line, lies at lower energy than that for the stripping component shown by a dashed line. The contribution of the stripping component to the total reaction cross section at

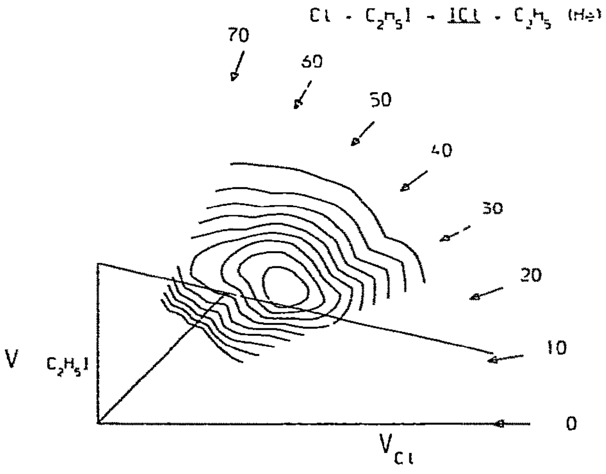

Fig. 3. Contour map of laboratory flux of ICl product from Cl + C_2H_5I at an initial translational energy $E = 56$ kJ mol^{-1} as a function of laboratory angle Θ and velocity v.

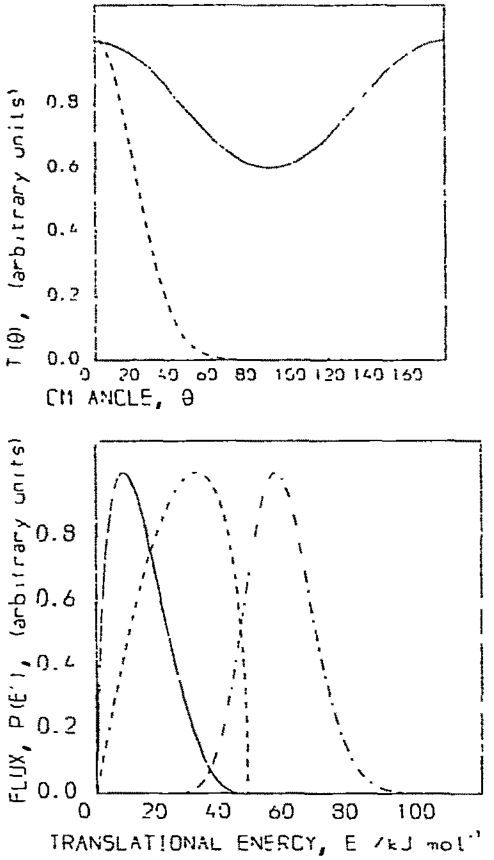

Fig. 4. Centre-of-mass angular distributions $T(\theta)$ and product translational energy distributions $P(E')$ obtained for Cl + C_2H_5I at an initial translational energy E = 56 kJ mol^{-1}. Solid lines for the long-lived complex component, broken lines for the stripping component and dot-dashed line for the distribution of initial translational energy.

this energy is estimated to be ≈10%. Scattering at the lowest collision energy for Cl + C_2H_5I showed only a long-lived complex, while the stripping component is just apparent at intermediate collision energy and becomes quite pronounced at the highest collision energy, as may be judged from the increasing asymmetry of the laboratory angular distributions shown in fig. 2. Similar centre-of-mass angular distributions $T(\theta)$ and product translational energy distributions $P(E')$ to those shown in fig. 4 were used in the analysis of the data for Cl + CH_3I. The long-lived complex alone fitted the data at lower and intermediate collision energy for Cl + CH_3I with the stripping component appearing only at the highest collision energy, as may be judged from fig. 1. Similar measurements have also been made on the Cl + C_3H_7I reaction. Both the long-lived complex and the stripping component are required to fit the data for Cl + C_3H_7I at all the collision energies but the stripping component becomes more prominent with increasing collision energy. The threshold function for Cl + CH_3I was determined [9] by measuring the total yield of ICl product as a function of collision energy. The resulting threshold energy E_{th} is listed in table 1 together with estimated values for the Cl + C_2H_5I, C_3H_7I reactions and the reaction exoergicities ΔD_0.

Table 1
Reaction energetics: translational threshold energy E_{th} and reaction exoergicity ΔD_0

Engergy (kJ mol^{-1})	CH_3I	C_2H_5I	C_3H_7I
E_{th}	19 ± 3	≈15	≈10
ΔD_0	−15 ± 3	−10	−5

4. Discussion

The long-lived collision dynamics observed at lower collision energy for each of these reactions is adequately described by the RRKM AM model [8] assuming that energy is randomised over all the internal modes of the complex allowing for the small quantum weighting of the H atoms [10]. However the osculating complex model [1] does not give a good description of the breakdown of the long-lived complex dynamics, since a sharply forward-peaked component emerges with a product translational energy distribution which lies well above that of the long-lived collision complex. It thus appears that direct stripping dynamics occur for collisions at the largest impact parameters where the high angular momentum of the collision impedes the reactive trajectory from exploring the well on the potential energy surface at small internuclear distances due to centrifugal repulsion. Energy exchange with internal modes of the collision complex, other than motion along the reaction coordinate, is thereby impeded and direct stripping dynamics results. However collisions at smaller impact parameters, which involve trajectories reaching the potential energy well, result in long-lived collision dynamics. This is very similar to the two-component mechanism proposed for the O + Cl_2 reaction [11] but the distinction between the stripping and long-lived complex components is more pronounced in the present case due to the larger number of internal modes provided by the alkyl radicals. Thus the distinction between the osculating complex model [1] and the two-component mechanism, though modest for the Cl + CH_3I reaction, is quite pronounced for Cl + C_2H_5I and C_3H_7I.

The high product translational energy of the direct stripping component may be attributed to the effect of a high centrifugal barrier for dissociation of the collision intermediate with a large initial orbital angular momentum L. If we assume that the long-range attraction varies as $V(r) \propto -1/r^6$ then the maximum barrier is given [9,12] by

$$B'_m \approx (\mu L'^2/\mu' L^2)^{3/2} E, \tag{2}$$

where μ, μ' denote the reactant and product reduced masses, E the initial translational energy and L' the final orbital angular momentum. Applying this formula to the peak product translational energy for Cl + C_2H_5I shown in fig. 4 indicates that $L' \approx \frac{3}{4}L$ and a similar value applies to Cl + C_3H_7I. However for Cl + CH_3I a lower fraction of the intitial orbital angular momentum is disposed into final orbital angular momentum $L' \approx \frac{1}{2}L$. As a consequence of the light mass of the CH_3 radical, a roughly equal fraction will be disposed into ICl product angular momentum $J' \approx \frac{1}{2}L$. However the scattering remains sharply forward-peaked because it arises from a near collinear transition state [4] and the vectors L' and J' both lie nearly parallel to L.

Indeed it is remarkable that ICl product scattering from a long-lived complex should be observed so close to the energy threshold for the endoergic Cl + CH_3I reaction. Application of RRKM theory [13] would indicate that the more energetically favourable dissociation of the collision complex back to reactants should be the dominant pathway. If however dissociation back to reactants disposes angular momentum primarily into orbital angular momentum while dissociation to product yields significant ICl product angular momentum, then a minimum angular momentum barrier may be raised in the exist valley and compensate to some extent for the endoergicity of the Cl + CH_3I potential energy surface.

Acknowledgement

Support of this work by Science and Engineering Research Council and by a NATO Grant to AGU is gratefully acknowledged.

References

[1] G.A. Fisk, J.D. McDonald and D.R. Herschbach, Discussions Faraday Soc. 44 (1967) 228.
[2] J.M. Farrar and Y.T. Lee, J. Chem. Phys. 63 (1975) 3639.
[3] D. Krajnovich, Z. Zang, F. Huisken, Y.R. Shen and Y.T. Lee, Physics of electronic and atomic collisions, ed. S. Datz (North-Holland, Amsterdam 1982) p. 733.
[4] S.M.A. Hoffmann, D.J. Smith and R. Grice, Mol. Phys. 49 (1983) 621.
[5] P.A. Gorry and R. Grice, J. Phys. E12 (1979) 857.
[6] C.V. Nowikow and R. Grice, J. Phys. E12 (1979) 515.
[7] E.A. Entemann, Ph.D. Thesis, Harvard University (1967).
[8] S.A. Safron, N.D. Weinstein, D.R. Herschbach and J.C. Tully, Chem. Phys. Letters 12 (1972) 564.
[9] S.M.A. Hoffmann, D.J. Smith, A. González Ureña and R. Grice, to be published.
[10] J.T. Cheung, J.D. McDonald and D.R. Herschbach, Faraday Discussions Chem. Soc. 55 (1973) 377.
[11] P.A. Gorry, C.V. Nowikow and R. Grice, Mol. Phys. 37 (1979) 347.
[12] L.D. Landau and E.M. Lifshitz, Mechanics, 2nd Ed. (Pergamon Press, Oxford, 1969) p. 51.
[13] W.B. Miller, S.A. Safron and D.R. Herschbach, J. Chem. Phys. 56 (1972) 3581.